AD-A191 575 RADIOGRAPHY OF LIQUID METAL FUEL COMBUSTION(U) NAVAL OCEAN SYSTEMS CENTER SAN DIEGO CA L A PARNELL ET AL. JAN 88 1/1

UNCLASSIFIED F/G 21/4 NL

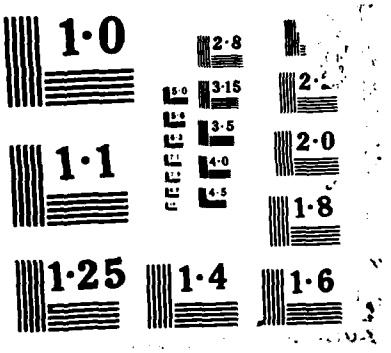
1·0
1·1
1·25
1·4
1·6
2·8
3·15
3·5
4·0
4·5
2·2
2·0
1·8

UNCLASSIFIED
SECURITY CLASSIFICATION OF THIS PAGE

DTIC FILE COPY

REPORT DOCUMENTATION PAGE

AD-A191 575

1b. RESTRICTIVE MARKINGS

3. DISTRIBUTION/AVAILABILITY OF REPORT

Approved for public release; distribution is unlimited.

4. PERFORMING ORGANIZATION REPORT NUMBER(S)

5. MONITORING ORGANIZATION REPORT NUMBER(S)

6a. NAME OF PERFORMING ORGANIZATION	6b. OFFICE SYMBOL (If applicable)	7a. NAME OF MONITORING ORGANIZATION
Naval Ocean Systems Center	NOSC	Naval Ocean Systems Center

6c. ADDRESS (City, State and ZIP Code)	7b. ADDRESS (City, State and ZIP Code)
San Diego, California 92152-5000	San Diego, California 92152-5000

8a. NAME OF FUNDING/SPONSORING ORGANIZATION	8b. OFFICE SYMBOL (If applicable)	9. PROCUREMENT INSTRUMENT IDENTIFICATION NUMBER
Office of Naval Research	ONR	

8c. ADDRESS (City, State and ZIP Code)	10. SOURCE OF FUNDING NUMBERS			
	PROGRAM ELEMENT NO.	PROJECT NO.	TASK NO.	AGENCY ACCESSION NO.
800 North Quincy Arlington, VA 22217-5000.	61153N	HM36	RR02403	DN305 145

11. TITLE (include Security Classification)

Radiography of Liquid Metal Fuel Combustion

12. PERSONAL AUTHOR(S)

L.A. Parnell, D.L. Katz, and J.T. Gilchrist

13a. TYPE OF REPORT	13b. TIME COVERED	14. DATE OF REPORT (Year, Month, Day)	15. PAGE COUNT
Professional paper	FROM Aug 1987 TO Aug 1987	January 1988	

16. SUPPLEMENTARY NOTATION

17. COSATI CODES			18. SUBJECT TERMS (Continue on reverse if necessary and identify by block number)
FIELD	GROUP	SUB-GROUP	Liquid metal fuels, jet-driven circulating energy conversion, X-ray radiography.

19. ABSTRACT (Continue on reverse if necessary and identify by block number)

Liquid metal fuels are being employed as Rankine cycle heat sources for undersea vehicle propulsion systems, necessitating investigation of the fundamental chemical, thermodynamic, and hydrodynamic processes which occur during the confined combustion of these fuels. Results of the development of techniques for this use of flash X-ray radiography to investigate these processes is presented. Experimental combustors designed to permit studies of the combustion zone and fluid dynamics of the jet-driven circulating flow in the fuel bath are described. Radiographic images showing the reaction zone, multiphase flow structures and the behavior and mixing characteristics of the products-rich phase are shown, demonstrating the utility of this experimental techniques in energy conversion research.

Presented at 22nd Intersociety Energy Conversion Engineering Conference, Philadelphia, PA; 10-14 August 1987.

20. DISTRIBUTION/AVAILABILITY OF ABSTRACT	21. ABSTRACT SECURITY CLASSIFICATION
☐ UNCLASSIFIED/UNLIMITED ☒ SAME AS RPT ☐ DTIC USERS	UNCLASSIFIED

22a. NAME OF RESPONSIBLE INDIVIDUAL	22b. TELEPHONE (include Area Code)	22c. OFFICE SYMBOL
L.A. Parnell	(619) 553-1588	Code 634

DD FORM 1473, 84 JAN

83 APR EDITION MAY BE USED UNTIL EXHAUSTED
ALL OTHER EDITIONS ARE OBSOLETE

UNCLASSIFIED
SECURITY CLASSIFICATION OF THIS PAGE

IECEC'87

IECEC'87
IECEC'87
IECEC'87
IECEC'87
IECEC'87
IECEC'87
IECEC'87
IECEC'87
IECEC'87
IECEC'87
IECEC'87
IECEC'87
IECEC'87
IECEC'87
IECEC'87
IECEC'87

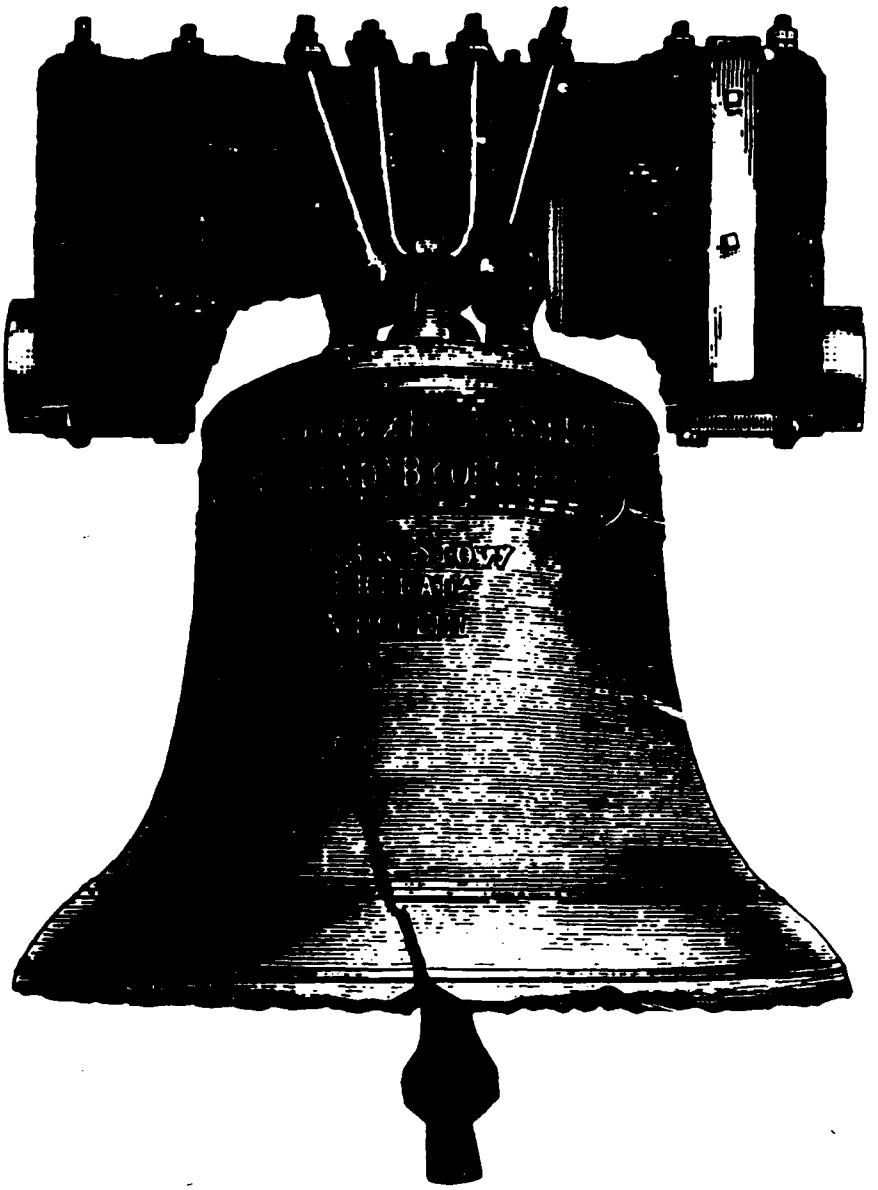

22nd ıtersociety Energy Conversion Engineering Conference

"ENERGY-NEW FRONTIERS"

August 10-14, 1987

RADIOGRAPHY OF LIQUID METAL FUEL COMBUSTION

L. A. Parnell, D. L. Katz and J. T. Gilchrist
Naval Ocean Systems Center
San Diego, California

L. E. Bryant, J. P. Lucero and W. D. Zerwekh
Los Alamos National Laboratory
Los Alamos, New Mexico

Abstract

Liquid metal fuels are being employed as Rankine cycle heat sources for undersea vehicle propulsion systems, necessitating investigation of the fundamental chemical, thermodynamic, and hydrodynamic processes which occur during the confined combustion of these fuels. Results of the development of techniques for the use of flash X-ray radiography to investigate these processes is presented. Experimental combustors designed to permit studies of the combustion zone and fluid dynamics of the jet-driven circulating flow in the fuel bath are described. Radiographic images showing the reaction zone, multiphase flow structures and the behavior and mixing characteristics of the products-rich phase are shown, demonstrating the utility of this experimental technique in energy conversion research.

Nomenclature

a	attenuation coefficient of object
a_o	attenuation coefficient of surrounding material
C	image contrast
C_o	object contrast
I	intensity, W/m^2
R	contrast ratio
Z	atomic number
x	X-ray path length, m
μ	mass attenuation coefficient
ρ	density, kg/m^3

Introduction

The search for increased energy density in thermal power cycles is a continuing need of the Navy's undersea vehicle research and development efforts.[1-4] The combustion of highly energetic, low density liquid metals is one of the approaches to advanced propulsion systems currently being pursued[2-5] and is the subject of the work reported here. Examination of the fundamental chemical, thermodynamic, and hydrodynamic processes present in such highly energy-dense heat sources requires special techniques due to the highly reactive and hostile nature of the reactants involved in such power sources.[6-8] To gain better understanding of such processes, we are investigating the reactions and the complex interactions which occur in closed, liquid metal combustion.

As the very reactive nature of alkaline metal fuels represents a considerable challenge to investigative measurements, we have been working on the development of new methods of studying the behavior of liquid metal combustion processes through the use of X-ray radiographic imaging technology. This paper reports work concentrated on the development of experimental diagnostics and imaging techniques in flash radiography to be used as investigative tools for analysis of the liquid-metal combustion phenomena mentioned. Imaging of combustion processes present when a jet of high molecular weight oxidizer is immersed in a liquid Li fuel bath has been done. Our focus in this work has been on the region where the reactions occur, determination of the size, locus and stability of this region, study of the overall flowfield structure in the combustion chamber and examination of the behavioral characteristics of the dense reaction products.

Radiographic Imaging

The applicability of the use of penetrating radiation for diagnostic studies of very energetic reactions of low-density fuels and gaseous oxidizers, requires examination prior to proceeding with this approach. The radiographic technique described in this paper was motivated by a simple theoretical analysis - the essentials of which are the subject of this section. After a presentation of the basic physics governing radiographic imaging and practical considerations for closed, liquid metal combustion, we conclude with a discussion of the technique used and a small but pertinent sample of results.

Theoretical Considerations

In X-ray radiography, images are the result of the differential attenuation of the beam by an object relative to its background; thus, it is the shadow projected by an object which is

recorded. The contrast ratio, R, is the ratio of the shadow brightness to background brightness and the contrast of the object is given by:

$$C_o = \frac{|1-R|}{1+R} . \quad (1)$$

Physically, C_o is the fractional deviation of the shadow brightness relative to the average brightness of the shadow plus background. Clearly, the detectability of a given image improves with increasing contrast, which is the single most important parameter in characterizing an imaging system. However, the ability to detect an image also improves with increasing image size and may also involve human factors such as association. Essentially, if the detection probability exceedes 1/2 then the image is considered detectable; for a given image size and shape there is a threshold contrast such that this condition is just satisfied.[9]

A useful expression for C_o follows from the exponential decay law for X-rays in matter.[10,11] Consider a uniform, parallel beam of monochromatic X-rays traversing a material medium. In a distance dx a fraction a·dx of the X-ray photons are removed from the beam by photoelectric absorption, Compton scattering into other directions and, for photon energies above 1.02 MeV, production of electron-positron pairs. Thus the beam penetration, I/I_o, obeys the exponential law $I/I_o = e^{-ax}$, where I_o is the initial beam intensity, I is the intensity after traversing a distance x in the medium and a is the linear attenuation coefficient. It should be emphasized that the beam is attenuated not by a gradual loss of energy by individual X-ray photons but instead by their gradual removal, in discrete events, from the beam. The linear attenuation coefficient is the product of the mass attenuation coefficient and density, $a = \mu\rho$. The mass attenuation coefficient, μ, is a function of atomic number and X-ray energy; for the X-ray energies of interest here, it is an increasing function of both atomic number, Z, and decreasing X-ray energy.[11] In case the material under analysis is a compound or mixture, the attenuation coefficient must be computed by averaging over the constituent elements and weighting the respective contributions according to the stoichiometry. Thus the constrast ratio for an object of thickness x in a medium with attenuation coefficient a_o is $R = e^{(a_o-a)x}$ and C_o is given by

$$C_o = \frac{|1 - e^{(a_o-a)x}}{1 + e^{(a_o-a)x}} . \quad (2)$$

Physically, the object introduces a spatial variation of the beam intensity which is then projected onto the recording medium. In the present case, a_o is the linear attenuation coefficient of the liquid Li. If the Li is displaced by a dense, high-Z material such as tungsten then the object will project a dark shadow on the recording medium. Conversely, the image of a void in Li would be brighter than the background; the part of the beam incident on the void arrives at the recording medium with an intensity $e^{a_o x}$ greater than that part not incident on the void. Thus, in effect, a void is an "object" which projects a bright shadow. If $C_o << 1$ it may be written, correct to first order, as:

$$C_o = \frac{|(a_o-a)x|}{2} . \quad (3)$$

Practical Considerations

In an experimental situation the combined effect of the cascaded elements of the X-ray system and other apparatus would be expected to result in some degree of contrast attenuation. If the resulting image contrast is C, then the contrast attenuation is just C/C_o. The image of a point object would be spread out into a two dimensional pattern known as the point spread function. Since the Fourier transform of a point is flat from zero to infinite spatial frequency, the normalized Fourier transform of the point spread function yields the response of the overall system to each component spatial frequency. The modulus of this Fourier transform is known as the Modulation Transfer Function (or MTF) and is none other than the contrast attenuation as a function of spatial frequency. In the present work, it has been assumed that the smallest images of interest are still large compared to the resolution limit of the system and therefore the MTF is taken to be constant. The object contrast, C_o, should be taken as the upper limit on the image contrast. Also, since the X-ray source would be polychromatic and the X-ray path length through the object might be variable, the object contrast would be more correctly computed by averaging the given expression over the X-ray spectrum and object thickness.

X-ray radiography provides a non-intrusive in-situ technique for flow visualization in liquid metal combustion. High contrast images of contemporaneous stainless steel objects being moved, deformed or destroyed in the presence of such combustion are easily obtained as are medium contrast images of the relatively dense product mixture, as shown by Parnell, et al.[12] More difficult to detect are images of small voids in a low-density alkaline metal such as Li; the difficulty arises principally because in order to penetrate the stainless steel containment walls of presently used liquid metal combustors, X-ray energies higher than those most suited for the imaging application must be employed. Nevertheless, there is evidence that a properly designed experiment can yield image contrasts above the detection threshold for small voids in Li; for example, film radiographs (described below) suggesting the outline of the combustion zone have been obtained, although perhaps aided by a fortuitous enhancement of the contrast due to the presence of condensed reaction products outlining the low-density zone.

Description of Experiments

The liquid metal combustion test apparatus and related instrumentation used for these experiments were located inside a reinforced concrete cell and monitered from an adjacent control room. Closed circuit television provided visual observation of the combustor during its operation. The combustor itself was mounted from a support shield and protruded into the path of the penetrating X-ray beam. A container housing the radiographic film and film changer was placed behind the combustor in line with the X-ray beam. Fig. 1 shows a schematic of the test cell, combustion apparatus and radiographic equipment assembled for testing.

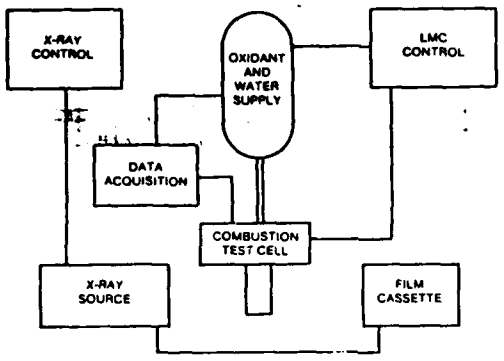

Fig. 1 Liquid metal combustion test facility and radiographic arrangement.

Combustor Design

Two containment vessels were designed to facilitate obtaining radiographic images which would permit study of the combustion zone. Prismatic configurations with moderately large aspect ratio, rectangular cross section combustion chambers were designed. These provided uniform attenuation of the radiation field throughout the field of view and eliminated distortion which is present in commonly-used cylindrical chambers due to curvature of the combustion chamber walls.

Each of the prismatic combustors constructed was made from stainless steel rectangular tubing cut and welded to form the desired cross section. They had integral heat exchangers and were mounted to standard pipe flanges for assembly and support as shown in Fig. 2. The internal cross-sections were 40 mm by 120 mm and 70 by 120 mm, respectively. Both were 320 mm long, providing for fuel capacities of 0.57 and 0.80 kg of Li, respectively. The shaded areas in Fig. 3 indicate the regions in which the combustion process and all reaction products were confined. The reaction containment walls of the combustors were made of AISI type 304 stainless steel in both cases. The wall thickness was 4.7 mm everywhere except for a 260 by 110 mm recessed region on either lateral face where material had been removed to reduce the thickness to 3.2 mm. The first combustor's heat exchanger incorporated 280 by 140 mm windows of 3.2-mm thick aluminum on each side to reduce X-ray attenuation (Fig. 3a). The second combustor had no provision to provide cooling of the lateral sides (other than natural convection) and thus represented the minimum attenuation to the penetrating radiation (Fig. 3b). The arrows in Fig. 3 indicate the path of the coolant during operation. Both combustor designs included a cap on one end which allowed for sealed thermocouple penetration into the bath and flanges at the other end containing an oxidant injection nozzle and fittings which allowed for the preparation and initiation of the experiments. The combustors were mounted in cantilever fashion from a support shield which separated them from the control and instrumentation hardware. The resulting material in the X-ray path due to the containment of the reaction and products was thus 6.4 mm of stainless steel and, for the first combustor, 6.4 mm of aluminum plus approximately 35 mm of water in the heat exchanger.

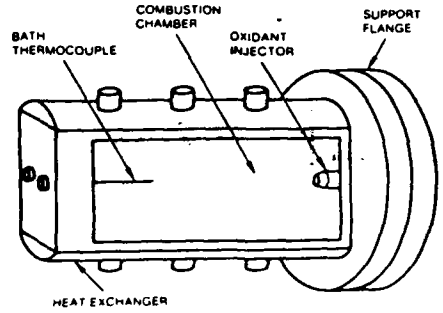

Fig. 2 Liquid metal combustor. Components as noted.

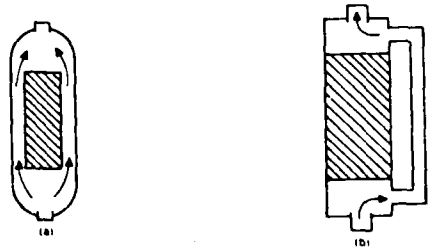

Fig. 3 Prismatic combustor cross sections. Coolant flow paths are indicated: (a) cooled on all sides; (b) cooled on upper and lower surfaces only.

Combustion Experiments

Prior to the start of each experiment fuel, typically one-half to one kilogram of Li, and a starting compound were placed in the combustor, the ullage was filled with oxidant and connections were made to the firing circuit for a pyrotechnic initiator. Radiographic equipment was then placed adjacent to the test device and a baseline X-ray was taken to confirm the operation and alignment of the X-ray equipment. The resulting baseline radiograph shows the injector, igniter and pyrotechnic charge within the voids cast into the Li fuel (cf. Fig. 4). Thermocouples on the exterior of the combustion chamber and in its center are also visible.

The experiments began by ignition of the pyrotechnic charge which melted the fuel and raised the bath temperature to a level which would sustain combustion. This was accompanied by commencing injection of the oxidant and initiation of the water flow through the heat exchanger, all three events being controlled by a pre-programmed timer. Pressure, temperature and flow data were acquired and digitally recorded to facilitate monitoring the combustor performance and for subsequent analysis.

Regulation and termination of the combustion process was done through control of oxidant flow through the injector nozzle. In the first experiment reported here the combustion process was sustained for 225 seconds until terminated due to a steady rise in oxidant injector pressure, such pressure rise indicating that combustion of the fuel was substantially complete. Fig. 5 shows the thermal response of the fuel bath and adjacent walls for this experiment. As the steady bath thermocouple response shows, the coolant flowrate chosen for this test was well matched with the power output of the reaction which can be as much as 400 kW for the reactions being investigated in this work. The second experiment was terminated after 45 seconds of operation (17% of the fuel consumed) with the bath temperature in excess of 1100 °C and the containing wall temperature over 1000 °C. This early termination was expected as the heat exchanger covered less than 40% of the containment surface

Fig. 4 Radiograph of combustor prior to initiation of reaction. Injector, thermocouples, fuel and pyrotechnic material are visible.

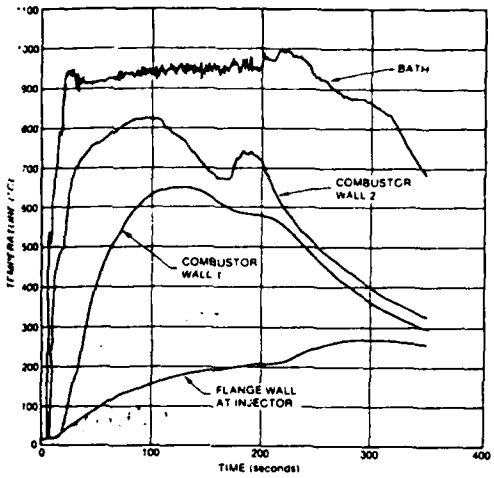

Fig. 5 Thermal response of fuel bath and adjacent walls. Combustor cooled on all sides.

area, providing no cooling at all on the lateral sides of the combustor, and the rate of heat removal was less than that produced by the reaction.

Radiographic Technique

The goal in developing this technique was to provide sequential radiographic images during the combustion process at an interval of 15 to 20 seconds in order to provide a sampling of the time history of the progression of the reaction zone during the experiment. The equipment selected was required to meet several challenging requirements: first, the combustion and circulation processes are dynamic, thus the image should be created as quickly as possible to prevent its blurring; secondly, the contrast of the object was low, so that the imaging medium should take advantage of all the contrast range available; finally, the combustor becomes very hot during the test and the recording medium cannot be in direct contact with it.

To meet the first of these goals, a 450 kV Hewlett Packard flash X-ray generator was used as the radiation source. It provides a radiation pulse of approximately 30 ns duration which is short enough to stop any motion of the reaction zone. Detuned to 375 kV, it provides sufficient energy to penetrate the combustor at a standoff distance sufficient to cause minimal geometric distortion and unsharpness of the image.

As no electronic imaging system could be found to meet the contrast requirement, industrial X-ray film with intensifying screens were used. After evaluating a number of film-screen combinations, Kodak AA film and Dupont NDT-9 screens were chosen as giving the best contrast ratio, R. In order to facilitate sequential exposures, an automatic film changer was developed to allow changing the film within the recharging time of the flash X-ray system. The changer uses 357-mm wide roll film, 460 mm per exposure and has supply and takeup reels with sufficient capacity for approximately 50 exposures. The changer also incorporates a pneumatic diaphragm to compress the intensifying screens tightly against the film during exposure while allowing retraction during the film change cycle. The film was developed in an industrial processor to allow processing the entire roll of film intact and to assure that the processing was uniform throughout the entire roll.

The radiographic setup employed a source to film distance of 110 cm and an object to film distance of 15 cm to provide minimal geometric unsharpness. During the experiments the radiographic procedure consisted of providing a baseline exposure before ignition as a geometric and density reference, an initial dynamic exposure at 100 ms after ignition, and recurring exposures every 15-18 s. A post-test exposure was also taken, again for reference purposes.

Radiographic Results

The liquid-metal combustion zone is potentially the most interesting, as well as the most difficult, feature to be imaged. Radiographically, this zone is essentially a void in liquid Li, which makes it an intrinsically low contrast "object." In order to maximize the contrast the lowest X-ray energy consistent with a reasonable level of penetration through the combustor is needed. The X-ray source described above, employing a tube voltage of a few hundred kV (yielding a nominal X-ray energy near 100 keV) is optimal. The sensitivity of the beam penetration to X-ray energy is demonstrated by the fact that the penetration through a single 3 mm stainless steel wall decreases from 53% at an X-ray energy of 124 keV to only 6% at 62 keV. In the table below, the object contrast at 124 keV for various objects in liquid Li is given. The necessary radiographic and physical data were taken, respectively, from Kaelble[11] and Kittel.[13]

Table 1 Object Contrast in Liquid Lithium

Material	Thickness (mm)	Contrast† (%)
Void	1	0.31
	10	3.1
	50	15.4
	100	30.0
Lithium	any	0
Reaction Product*	1	1.06
	10	10.6
	50	48.7
	100	78.8
Steel	1	10.1
	5	46.7
	10	76.7
Tungsten	0.1	27.2
	1	99.2
	2	99.9

† X-ray energy = 124 keV

* Density = 1.9 gm/cm³

Immediate separation of the reaction products into an immiscible fluid volume below the injection point was noted during all of the tests and has been reported elsewhere.[11] Figs. 6 and 7 are radiographs which show the development of the settled product volume as the reaction proceeds towards complete consumption of the fuel. Fig. 6, taken approximately 3 s after the start of combustion, shows gas dispersed throughout the liquid Li in most of the chamber and predominantly gaseous regions in front of the injector and in the upper right quadrant of the chamber. Three external thermocouples and a single interior sheathed one are visible and provide known-contrast references. Evidence of an established fluid circulation pattern is not visible in this radiograph, possibly due to residual dispersion of gases which occurs during initiation of the combustion process.

Fig. 6 Radiograph of combustion process after operating for 3 s. Uniform mixing of fuel and vapor is shown. Gaseous regions in front of and above injector can be seen.

The radiograph shown in Fig. 7 was taken 19 s after initiation of the reaction and clearly shows a separated dense-product volume, although only about 10% of the fuel had been consumed at that time. This volume, seen as a dark mound beneath the injector whose height increases as it nears the oxidizer source, indicates some turbulent interaction at the Li-product interface. The liquid Li region in the lower left quadrant of this image contains less dispersed gas than is the case in Fig. 6; a considerably greater proportion of the combustion chamber volume appears to be gaseous in Fig. 7 as well. There are turbulence structures in this radiograph in both the liquid and predominantly-gaseous phases of the flowfield. Additionally, there is some indication of a continuous gaseous jet originating at the injector and extending about 60% of the length of the combustion chamber. It is interesting to note from this radiograph that three distinct and somewhat separated fluid regions can be present in the early stages of the combustion process: a dense product region which grows as the fuel is consumed; a less dense fuel-rich region below the oxidizer jet; and a dispersed-gas region in which the combustion and condensation processes appear to be primarily confined.

Fig. 7 Radiograph of combustion process after 19 s operation. Regions of dense products, fuel-rich and gas-liquid phases can be distinguished.

Several distinct gaseous cells are visible in Fig. 8 at the upper right boundary of the combustion chamber, which we infer to be due to recirculation. This figure is a radiograph of the first combustor described above in which cooling was provided on all sides of the reaction chamber; the image was taken 33 s after the start of combustion, showing the state in that chamber after approximately 24% of the fuel had been consumed. The apparently well-mixed combustion region and the separated dense product volume are easily distinguished. A turbulent shear flow interface between these two features can be seen, but a separate fuel-only phase is not present. The height of the dense products layer can be seen to reach the center of the combustor at the oxidizer injector and a wave-like structure is present at the surface of the layer, indicating substantial entrainment from the products layer by the gaseous jet. For the fuel-oxidizer combination selected for these experiments it is evident from Figs. 7 and 8 that gravitational effects dominate the behavior of the liquid reaction products in the bath, causing their separation from the fuel and gases until their entrainment from the products layer by the oxidizer jet is forced by growth in the volume of this dense phase.

Fig. 8 Radiograph of combustion process after 33 s operation. Chamber cooled on all sides. Distinct gaseous recirculation cells, well-mixed combustion region and dense product volume are visible.

Concluding Remarks

Results of tests using prismatic combustors which have single, horizontal oxidizer jets at their centers have been presented. Separation and growth of the reaction products into a product-rich dense fluid volume below the injection point is observed. Radiographs show a reduced volume for the violently mixed fuel-vapor region in which the combustion processes appear to be confined. Evidence of a third, contiguous fuel-rich phase was also observed while most of the fuel remains unused. Radiographic evidence of the oxidizing jet is presented to indicate the stability, envelope and growth rate of the reaction zone. These results show that studies of the combustion processes of confined, very reactive low-density fuels at high temperatures can be performed successfully through the use of carefully selected flash X-ray techniques, affording the investigator with the opportunity to gain increased understanding of the behavior of these very energetic heat sources.

Acknowledgements - This work was funded in part by the Naval Ocean Systems Center Independent Research Program and in part by the Office of Naval Research.

REFERENCES

1. J. N. Matavi, F. E. Heffner and A. A. Miklos, *SAE Trans.*, 78, 2376 (1969).
2. W. L. N. van der Sluys, *Proc. Tenth Intersociety Energy Conference*, 1031 (1975).
3. U. K. P. Biermann, *ibid.*, 1023 (1975).
4. E. G. Groff and G. M. Faeth, *J. Hydronautics*, 13, 63 (1978).
5. J. F. Avery and G. M. Faeth, *Fifteenth Symposium (International) on Combustion*, The Combustion Institute, Pittsburgh, 501 (1975).
6. L-D. Chen and G. M. Faeth, *Combustion Science and Technology*, 31, 277 (1983).
7. D. A. Greene, *Liquid Metal Engineering and Technology*, BNES, London, 13 (1984).
8. D. H. Cho, D. R. Armstrong and L. Bova, Argonne Nat. Lab. Report No. ANL-886-41 (1986).
9. N. Jensen, *Optical and Photographic Reconnaissance Systems*, Wiley, New York (1968).
10. J. D. McGervey, *Introduction to Modern Physics*, Academic Press, New York (1971).
11. E. Kaelble, *Handbook of X-Rays*, McGraw-Hill, New York (1967).
12. L. A. Parnell, D. G. Edmunds and D. J. Rogerson, *Proc. AIAA/ASEE/ASME/SAE 23rd Joint Propulsion Conference*, San Diego, California (1987).
13. C. Kittel, *Introduction to Solid State Physics*, Wiley, New York (1976).

END

DATE

FILMED

5-88

DTIC